

## Pharmacological Evaluation of Humanized Anti-Epidermal Growth Factor Receptor, Monoclonal Antibody h-R3, in Patients With Advanced Epithelial-Derived Cancer

\*Tania Crombet, †Leonel Torres, ‡Elia Neninger, §Mauricio Catalá, †María E. Solano, †Alejandro Perera, \*Olga Torres, \*Normando Iznaga, \*Franz Torres, \*Rolando Pérez, and \*Agustín Lage

\*Center of Molecular Immunology; †Center for Clinical Research; ‡Hermanos Ameijeiras Hospital; §Center for Medical and Surgical Research, Havana, Cuba.

---

**Summary:** Epidermal growth factor receptor (EGFR) overexpression has been detected in many tumors of epithelial origin, and it is often associated with tumor growth advantages and poor prognosis. h-R3 is a genetically engineered humanized antibody (mAb) that recognizes an epitope located in the extracellular domain of human EGFR. The antibody exhibited potent *in vitro* and *in vivo* antitumor effect on EGFR overexpressing cell lines. To study safety, pharmacokinetics, and biodistribution, 12 patients with advanced epithelial-derived tumors received single intravenous infusion of h-R3 at four dose levels. Safety evaluation was made according to World Health Organization toxicity criteria. For biodistribution, 3 mg of the total dose were labeled with <sup>99m</sup>Tc-Technetium and then pooled with the rest of the dose. Anterior and posterior whole-body images were acquired using a gamma camera. Blood samples were taken for pharmacokinetics, antiidiotypic response, and for soluble EGFR detection. After hR3 administration, no evidence of severe toxicity was observed. Secondary reactions were mild and moderate and mainly consisted of tremors, fever, and vomiting. No anaphylactic or skin reactions were detected. Qualitative analysis of whole-body images showed that the liver had the highest mAb uptake. Pharmacokinetic analysis revealed that elimination half-lives and the AUC increased linearly with dose, while total body clearance decreased when increasing doses of h-R3. No relation between shed EGFR and mAb clearance was found. No antiidiotypic response against h-R3 was detected. Several phase II trials are now underway to evaluate the efficacy of h-R3 in the treatment of advanced cancer patients. **Key Words:** Epidermal growth factor receptor—Monoclonal antibody—Phase I clinical trial.

---

The epidermal growth factor receptor (EGFR) is a transmembrane glycoprotein mediating mitogenic effects on epithelial cells. It is overexpressed in a wide variety of human tumors, including nonsmall cell lung cancer (1,2), astrocytic tumors (3,4), head and neck (5,6), ovarian (7),

cervical (8,9), bladder (10), and esophageal cancers (11,12). EGFR has been associated with high malignant degree and poor outcome of cancer patients. More recently, EGFR expression has been correlated with alterations in cell cycle progression (13), increased invasive capacity (14), enhanced angiogenesis (15,16), and decreased apoptosis of tumor cells (17).

Several strategies have been developed to disrupt the EGFR-associated signal transduction cascade. The main therapeutic approaches include monoclonal antibodies (mAb) (18,19) directed against the extracellular binding

---

Received June 28, 2002; accepted November 7, 2002.

Address correspondence and reprint requests to Tania Crombet-Ramos, MD, Center of Molecular Immunology, Division of Clinical Immunology, P.O. Box 16040, Havana 11600, Cuba; e-mail: taniac@ict.cim.sld.cu

domain of the receptor and small molecule tyrosine kinase inhibitors (20), which act by interfering with ATP binding to the receptor.

Ior egf/r3 is a murine mAb obtained at the Center of Molecular Immunology (CIM) using the standard hybridoma technology, after immunization of BALB/c mice with a purified fraction of human placenta enriched in EGFR. The antibody recognizes EGFR with high affinity, inhibiting *in vitro* and *in vivo* proliferation of EGFR overexpressing cell lines (21,22).

Fifty-eight advanced cancer patients were treated with the referred murine mAb at doses from 160 to 3,200 mg, cumulative dose (23,24). After repeated exposure to ior egf/r3, anaphylactic reactions were detected in four patients, probably related with the development of human anti-mouse antibodies (HAMA) response. Pharmacokinetics demonstrated that the elimination half-life and the area under the time-concentration curve of the murine mAb increased linearly with the dose. Elimination half-life ranged from 27.3 hours for 50 mg to 65.89 hours for 500 mg (24). In parallel, 148 patients were included in immunoscintigraphic studies with the same antibody, at a low dose, labeled  $^{99m}\text{Tc}$  (25). Overall sensitivity of the immunoscintigraphic imaging was 84.2% for *in vivo* detection of primary tumors, metastases, and recurrences of many different epithelial neoplasms (25). No other similar study has been reported for any anti-EGFR mAb.

Ior egf/r3 was humanized by complementarity determining regions grafting into a human framework, to avoid immune response against the murine antibody and to improve its immunologic effector functions (26).

h-R3, the humanized mAb derived from ior egf/r3, is a genetically engineered IgG<sub>1</sub>, with high affinity ( $K_D = 10^{-9}$  mol/L) and specificity to the EGFR that blocks growth-factor binding receptor activation and subsequent signal-transduction events (27).

The antiproliferative and antiangiogenic effects of h-R3 were demonstrated *in vitro* as well as *in vivo* on the vulvar carcinoma cell line A431. In addition, a significant proapoptotic activity was shown *in vivo*, after the induction of complete regression of well-established human cancer xenografts. Flow cytometric analysis revealed that h-R3 arrest cell cycle progression at the G1/S boundaries (28).

To evaluate the tolerability, biodistribution, pharmacokinetics, and immunogenicity of h-R3, an open-label, dose-escalation phase I clinical trial was carried out in patients with advanced epithelial-derived tumors.

## MATERIALS AND METHODS

### Trial Design and Treatment Procedure

Twelve patients were included in four treatment cohorts (three patients each), receiving a single administration of the antibody. A modified Fibonacci scheme was used for dose escalation. The starting dose was selected taking into account the mAb effective dose at the experiments with human tumors xenografts (27,28) and considering that doses above 40 mg of another anti-EGFR mAb induced significant saturation of the target receptor within the tumor (29). mAb doses in the four defined groups were 50, 100, 200, and 400 mg. The antibody was administered by intravenous (IV) infusions, in 250 mL of sodium chloride, over 30 minutes. The Institutional Review Boards of the Center for Surgical and Medical Research, the "Hermanos Ameijeiras Hospital," and the Center for Clinical Research, hospitals in which the trial was carried out, approved the protocol. The State's Center for Drug Quality Control (CECMED), the National Regulatory Agency, also approved the protocol.

### Patient Selection

Patients with histologically confirmed advanced-stage epithelial tumors that were not amenable to receive any further therapy and who had finished their last treatment at least 4 weeks before were included in the trial. Other selection criteria were a good performance status, normal hematological conditions, as well as conserved hepatic and renal functions. The most important exclusion criteria consisted of previous treatments with murine anti-EGFR antibodies, pregnancy or lactation, serious chronic diseases, and active infections. All patients signed a written consent form before their inclusion in the clinical trial.

### Safety and Tolerability

Adverse reactions were detected by physical examination every 4 hours during the infusion day and then daily, up to 72 hours after h-R3 administration. In addition, patients underwent complete blood count including differential leukocyte count, platelet count, and hemoglobin. Other biochemical parameters such as total proteins, albumin, bilirubin, glucose, creatinine, and enzymes including glutamic oxalacetic transaminase, glutamic-pyruvic transaminase, and alkaline phosphatase were also measured. All laboratory tests were done before inclusion in the trial, then weekly for the first month and there after, monthly up to 6 months. Adverse events were

classified according to the World Health Organization (WHO) Toxicity Scale (30).

### **Biodistribution Study**

#### *Antibody Labeling and Quality Control*

h-R3 was directly labeled according to the Schwartz and Steinstrasser's method (31) as described previously (32,33). Labeled product was subjected to ascending paper chromatography on Whatman 3 MM paper as stationary phase and 0.9% saline and acetone as mobile phases for the radiochemical purity control. Radiochemical purity higher than 90% was considered satisfactory for patient administration.

Three milligrams of the total antibody dose were labeled with  $^{99m}\text{Tc}$  and were pooled with the rest of the unlabeled mAb, for all dosage groups to enable the assessment of biodistribution in vivo. The labeled antibody was used as a tracer for biodistribution purposes.

#### **Antibody Immunoreactivity**

A homogeneous radio receptor analysis (34) was used to measure the ability of the reduced mAb to interact with the EGFR expressed in a human placenta microsomal fraction. Reduced mAb was compared with nonreduced (native) antibody for its ability to compete with radiiodinated human EGF ( $^{125}\text{I}$ -EGF). Data from three independent experiments were averaged and plotted, showing that the reduction process had no effect on mAb immunoreactivity. Previously, similar results were obtained for  $^{99m}\text{Tc}$ -labeled h-R3 compared with nonreduced, control antibody after using the same radiolabeling procedure (32,33).

#### **Image Acquisition**

Anterior and posterior whole-body images were acquired at 10 minutes, 1, 3, 5, and 24 hours after mAb infusion, using a gamma camera (SOPHYCAMMERA DS7, France). The gamma camera head was fitted with a diverging parallel-hole collimator to increase the lateral viewing aspect. A 20% window centered on the 140 keV emission peak of the  $^{99m}\text{Tc}$  was used. All views were acquired at a speed of 20 cm/min using a 512 × 1024 matrix, zoom 1.

Images were processed in a SOPHY-20P system using the software BioDose v1.0, developed at the Center for Clinical Research. Geometric mean images were computed from the anterior and posterior whole-body scans and regions of interest were drawn over organs with

higher mAb uptake. Total counts were computed for the selected organs at different time intervals. Then, organ count values were converted to activity, corrected for decay and expressed as percentage of the total administered activity. Whole-body activity was initially 100%, followed by an exponential clearance due to biologic removal and physical decay of activity. No planar or single photon emission computed tomography images were acquired over the known disease sites.

#### **Pharmacokinetics Analysis**

Following antibody infusion, 3 mL of blood samples were collected in patients from an antecubital vein, opposite to the injection site, using an indwelling catheter at the following time intervals: 5, 10, 20, 30 minutes, 1, 3, 5, 8, 18, 24, 36, 48, 72, 168, and 720 hours after injection.

Counting radioactivity in serum to estimate antibody concentration was not useful, due to the short physical half-life of the isotope selected for the biodistribution assessment. The physical half-life of technetium ( $t_{1/2} = 6.02$  hours) was too short for optimal pairing with h-R3, resulting in an underestimation of the antibody clearance. To overcome this technical problem, a cellular ELISA was developed to estimate the serum antibody concentration. Briefly, A431 ( $10^4$  cells/well), an established overexpressing EGFR cell line, was plated into 96 wells culture plates. The cells were maintained at 37°C until confluence and formaldehyde 1% (50  $\mu\text{L}$ /well) was added to fix cells to the plate solid phase. Serial dilutions of h-R3 together with serum samples were added in triplicates. Plates were incubated for 1 hour at 37°C and, after washing, were incubated with an alkaline phosphatase-labeled anti-human IgG conjugate (Sigma Chemical Co, U.S.A.) at 37°C for 1 hour. Color was developed by adding 1 mg/mL of para-nitro-phenyl-phosphate diluted in diethanolamine buffer. Absorbance was read at 405 nm.

Pharmacokinetics was evaluated using model-dependent analyses performed according to the Akaike's Information Criteria (AIC) (35) as a statistical test by a software package (WIN NONLINE, MD, U.S.A.), which performs a nonlinear least squares regression analysis. All statistical analyses were performed using the SPSS software, version 8.0 (SPSS Inc, Chicago, IL, U.S.A.).

#### **Determination of Serum EGFR Level**

To evaluate the impact of shed EGFR in mAb clearance, the level of EGFR extracellular domain (ECD) in the pretreatment serum samples was measured, using a

commercial quantitative kit (Oncogene Science, Uniondale, NY, U.S.A.). The sandwich ELISA uses a capture mAb and an alkaline phosphatase-labeled mouse antibody as detector. Capture and detector antibodies recognize the ECD of EGFR. The ELISA was performed according to the manufacturer's recommendation. A positive elevation of serum EGFR level was defined as any value above the upper limit for healthy subjects.

### Antiidiotypic Response

Blood samples were collected at 0 and 7 days and then monthly up to 6 months, to detect antibodies that react with the murine ior egf/r3 idio type. A qualitative direct ELISA was performed by first coating high binding ELISA plates (Maxisorb; Costar, Cambridge, MA, U.S.A.) with ior egf/r3 (10 µg/mL) overnight at 4°C. Plates were washed and 1:100 dilutions of sera from h-R3-treated patients were added. Plates were incubated for 1 hour at 37°C and washed after an Alkaline Phosphatase coupled anti-human IgG antibody (Sigma Chemical Co) was added. Plates were incubated and washed and substrate (para-nitro-phenyl-phosphate, 1 mg/mL) was added. Absorbance was measured at 405 nm. A pretreatment serum sample of each patient was used as control. The assay was considered positive, when posttreatment/pretreatment ratio was higher than 2.

The sera working dilution was selected by making a dilution-absorbance calibration curve of a positive sample (from a treated patient) in parallel with the pre-

treatment sample. The working dilution was defined as the one in which the ratio between the positive and pre-treatment sample was the highest. Absorbance of the positive sample was measured in the section of the standard curve that exhibited a linear relationship between absorbance and dilution.

## RESULTS

### Patient Characteristics

Twelve patients, 1 man and 11 women, mean age 59 years (35 to 74 years), were enrolled in the trial; all had histologically confirmed advanced-stage epithelial tumors.

Primary tumors corresponded to ovary (four cases), breast (four cases), lung (two cases), stomach (one case), and kidney (one case). Patients were not eligible for any further treatment: five had previous surgery in combination with radiation and/or chemotherapy, two patients were treated with radio and chemotherapy, and four patients received radiotherapy or surgery alone, while one patient received chemotherapy exclusively. Patient characteristics are detailed in Table 1.

### Safety and Tolerability

No evidences of serious adverse events were observed. Seven of 12 patients (58.3%) developed mild or moderate adverse reactions according to the WHO toxicity

**TABLE 1.** Patients' baseline characteristics and adverse events after h-R3 treatment

Patient no.	Dose level, mg	Age, y/sex	Entry diagnoses	Stage	Previous treatment	Adverse events	Intensity (grade)
1	50	35/F	Ovarian adenocarcinoma	IV	Chemotherapy	Nausea and vomiting	1
2	50	50/F	Ovarian adenocarcinoma	IV	Surgery Chemotherapy	Fever, tremors, dryness of mouth	1
3	50	53/M	Lung epidermoid carcinoma	III	Radiotherapy Chemotherapy	Fever, flushing	1
4	100	68/F	Stomach adenocarcinoma	IV	Surgery	Tremors	2
5	100	58/F	Ductal infiltrating carcinoma of the breast	IV	Radiotherapy Chemotherapy	Tremors, asthenia	1
6	100	66/F	Ductal infiltrating carcinoma of the breast	IV	Surgery	No	
7	200	65/F	Ovarian adenocarcinoma	IV	Surgery Radiotherapy Chemotherapy	No	
8	200	68/F	Ductal infiltrating carcinoma of the breast	IV	Radiotherapy	No	
9	200	55/F	Lung epidermoid carcinoma	IV	Radiotherapy	No	
10	400	74/F	Ovarian adenocarcinoma	III	Surgery Radiotherapy	Tremors	2
11	400	58/F	Renal cell carcinoma	IV	Surgery Chemotherapy	Tremors, hypertension	2
12	400	62/F	Ductal infiltrating carcinoma of the breast	IV	Surgery Chemotherapy Radiotherapy	No	No

scale. All adverse events appeared between 30 minutes and 1 hour after infusion completion and were controlled with standard medication. Adverse reactions mainly consisted of tremors, fever, vomiting, nausea, dryness of mouth, asthenia, hypertension, and flushing. No acneiform rash or other dermatological toxicity was detected. Adverse events are described in Table 1.

### Biodistribution

The relative biodistribution of the antibody was expressed as the percentage of the injected dose (ID) in different organs at 5 time intervals. Time courses of radioactivity showed close similarities between individual patients at the same dose level. The results of the relative accumulation per organ and per dose levels at 1 and 24 hours after mAb infusion are given in Table 2.

A high background activity was present in the scintigraphic images during the first 5 hours, due to the slow blood clearance of h-R3.

The whole-body images revealed mAb accumulation in the liver, heart, kidneys, urinary bladder, and spleen through all time intervals. Two serial whole-body images are depicted in Figures 1A and B.

The liver showed a statically significant high accumulation in comparison with the rest of the body for the four doses. The activity was accrued in this organ immediately after the injection, reaching a maximum value within the first hour.

Antibody uptake was also evident in the large intestine of five patients. The activity imaged at this organ was visualized only 24 hours after mAb administration. For the rest of the patients, the activity in colon was probably eliminated before the acquisition of the late images. On the contrary, kidneys and urinary bladder were imaged in all patients within the first hour after mAb administration. The percentage of uptake in kidneys and urinary

bladder largely varied according to patients' urinary evacuation. In general, the antibody uptake decreased with time in all organs, except for kidneys, urinary bladder, and the gastrointestinal tract, which represent the excretion pathway of the antibody.

Five of 12 patients had at least one focus of moderate to high activity at a known disease site. There was no clear relation between mAb dose and tumor visualization since positive images were found almost at all dosage levels, excluding the second treatment cohort (100 mg). Primary tumors as well as extrahepatic metastases showed moderate to high uptake, while liver metastases were photopenic. Positive images corresponded to different tumors histology and were evident in patients 1, 2, 7, 9, and 11.

The biologic antibody clearance was compared between tumors and normal tissues as determined by the whole-body scans. Figure 2 represents h-R3 clearance, expressed as percentage of injected dose per gram of tissue (ID/g) in the tumor, in comparison with the liver and the heart for all patients showing positive uptake at the primary tumor. The percent of ID/g of tissue was significantly higher at the tumor than in the liver and the vascular pool. Furthermore, the percent of ID/g of tissue decreased after 24 hours posttreatment for normal organs, while the uptake in the tumor remained relatively constant.

### Pharmacokinetics

Pharmacokinetics parameters were obtained from ten patients. In two patients, blood sampling over the indwelling catheter was not possible, as a consequence of previous heavy chemotherapy.

Plasma disappearance curves of the humanized anti-EGFR mAb were best fit by bi-exponential equation with an elimination half-life ( $t_{1/2\beta}$ ) of 62.91, 82.60, 302.95,

**TABLE 2.** *h-R3 biodistribution in patients expressed as percent of the injected dose at 1 and 24 hours after mAb administration*

Source organ	Time, hrs.	% of injected dose			
		50 mg	100 mg	200 mg	400 mg
Heart	1	4.76 ± 0.7	5.84 ± 1.0	3.61 ± 0.6	4.07 ± 1.6
	24	1.12 ± 0.3	1.98 ± 0.78	1.71 ± 0.9	1.94 ± 1.1
Liver	1	24.76 ± 10.8	11.79 ± 2.5	9.88 ± 3.7	10.58 ± 0.9
	24	12.78 ± 4.9	10.35 ± 2.3	5.57 ± 3.8	5.98 ± 3.0
Spleen	1	0.96 ± 0.8	1.74 ± 0.1	1.58 ± 0.6	1.33 ± 0.1
	24	0.27 ± 0.03	1.03 ± 0.6	0.80 ± 0.4	0.69 ± 0.3
Kidneys	1	2.66 ± 0.6	2.46 ± 1.1	2.49 ± 0.2	3.04 ± 1.0
	24	11.02 ± 2.5	5.94 ± 4.8	8.82 ± 7.7	8.62 ± 1.6
Urinary bladder	1	1.37 ± 0.3	25.21 ± 4.1	4.21 ± 1.4	3.29 ± 1.4
	24	0.92 ± 0.8	4.34 ± 3.3	2.16 ± 1.3	3.04 ± 1.0

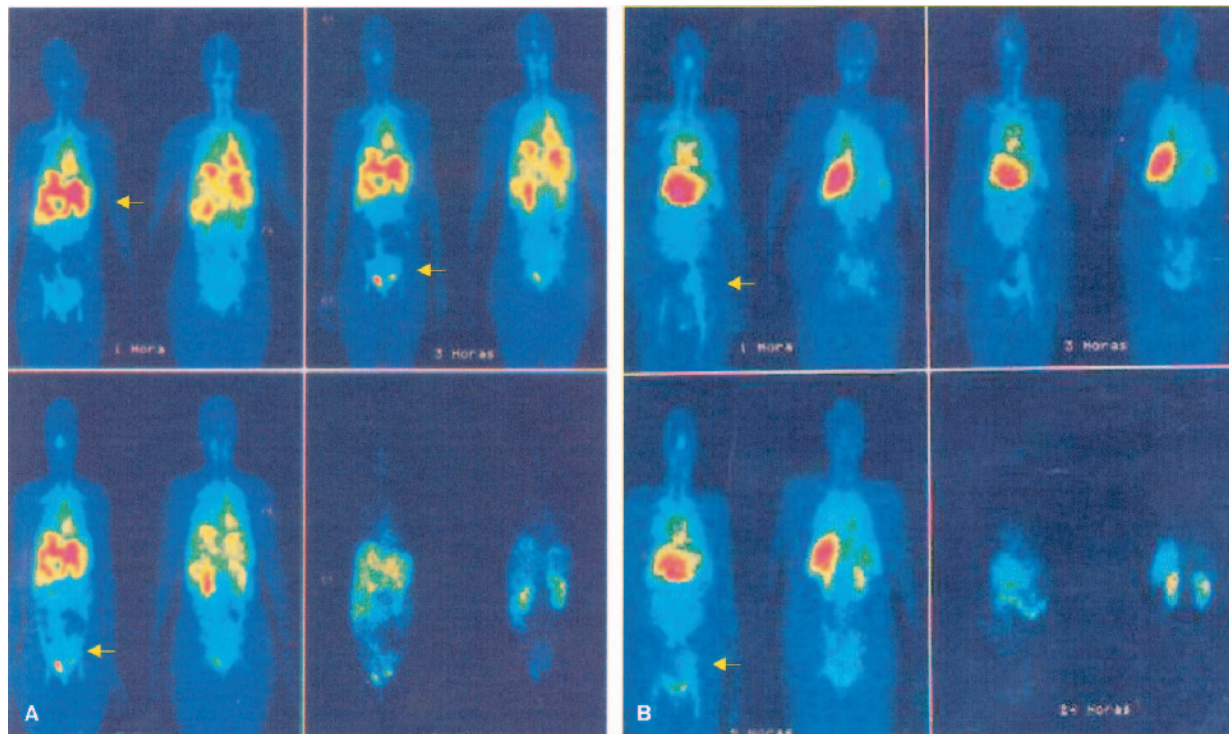


**FIG. 1.** (A and B) Serial anterior and posterior whole-body images of patients 1 and 2. Images were acquired at 1, 3, 5, and 24 hours after <sup>99</sup>Tc h-R3 infusion and showed mAb accumulation in the liver, heart, spleen, kidneys, and urinary bladder. Patient 1 had one focus of high activity in the ovarian primary tumor (left ovary) and multiple liver metastases that were photopenic. Patient 2 had one focus of high activity in the ovarian primary tumor (left ovary).

and 304.51 hours for the dose of 50, 100, 200, and 400 mg, respectively. The AUC was 45/458, 145/931, 573/612, and 635/275 ng/mL/min, and the maximal activity concentration ( $C_{max}$ ) was 27/790, 36/612, 52/713,

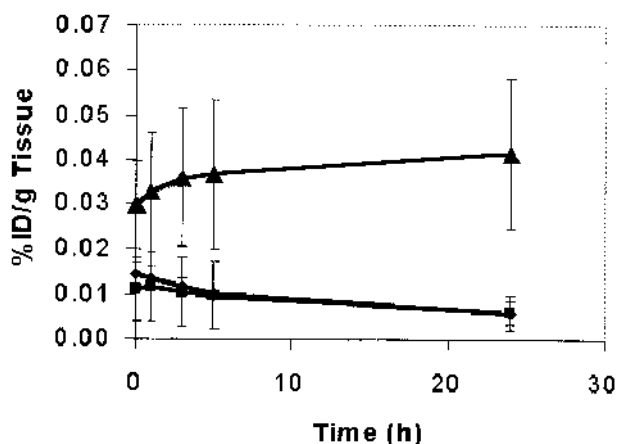


**FIG. 2.** Antibody clearance in tumor, liver, and heart, as determined by whole-body scans in a gamma camera expressed as Log % ID/g of tissue (tumor = 2 g, liver = 1,800 g, and heart = 330 g). The percentage of ID/g of tumor showed a greater variability than the percent of ID/g of normal tissues due to the diversity of the neoplasms showing mAb uptake. ◆ = Heart; ■ = Liver; ▲ = Tumor.

57/117 ng/mL for the dose of 50, 100, 200, and 400 mg, respectively. The apparent volume of the central compartment ( $V_c$ ) was 2321.96, 2823.67, 4279.71, and 7173.99 mL, and the total elimination clearance (Cl) was 1.08, 0.67, 0.34, and 0.76 (mL/hr/kg) for the dose of 50, 100, 200, and 400 mg, respectively. No statistically significant differences in clearance for the four dose levels were found ( $P = 0.095$ , Kruskal-Wallis Test).

**Determination of Serum EGFR Level**

EGFR level was quantified before inclusion in the clinical trial, using a human EGFR quantitative kit, to correlate pharmacokinetics with the soluble blocking antigen.

Since according to the kit information, the mean serum level of EGFR in the healthy population is 61 ng/mL (range 48–72 ng/mL), the cutoff value for EGFR positivity was 72 ng/mL. Positive serum elevation of EGFR was observed in 4 of 12 patients included in the study. Unexpectedly, the peak amounts of the soluble EGFR were detected in three patients bearing ductal infiltrating carcinomas of the breast (Fig. 3). No correlation was found between clearance and shed receptor.

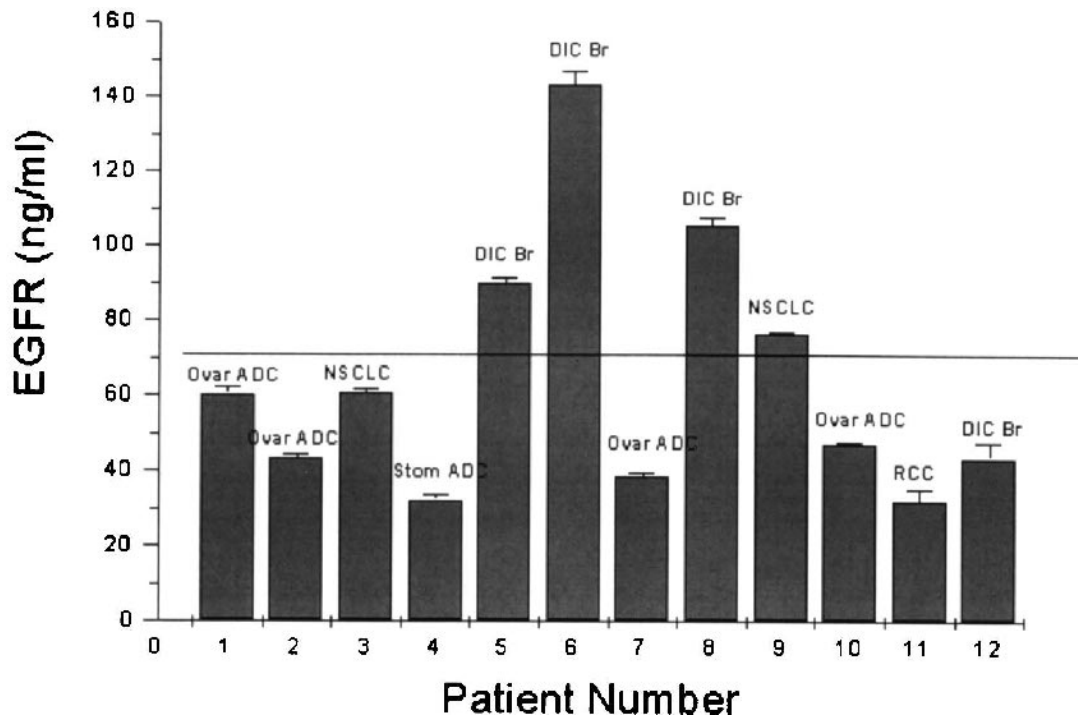


FIG. 3. Serum EGFR level in patients before treatment with h-R3.

### Antiidiotypic Response

No patient had detectable antiidiotypic antibodies after one infusion of h-R3 at any dosage level, with measurements performed up to 6 months after h-R3 treatment.

### DISCUSSION

Despite the advances in surgery, radiation, and chemotherapy, advanced epithelial-derived cancer largely represents an unsolved problem. Today, biologic therapy emerges as the fourth modality for cancer management, being a very attractive option taking into consideration its specificity and low toxicity (36). Passive immunotherapy against solid tumors with naked antibodies has recently demonstrated efficacy in the clinical setting (36).

EGFR is a very attractive target for immunotherapy since EGFR driven autocrine growth pathway has been implicated in the development and progression of the majority of human epithelial cancers (37).

We report the results of a single-dose escalation study of the humanized anti-EGFR mAb h-R3 in advanced cancer patients. The trial was designed to evaluate h-R3 safety, pharmacokinetics, biodistribution, and immunogenicity.

After a single injection, h-R3 was very well tolerated.

No dose-limiting toxicity was observed, and, therefore, the maximum-tolerated dose was not reached. The adverse events appeared immediately after the mAb administration and were considered infusion reactions. Infusion related events have been previously described in clinical trials with high doses of other antibodies like Herceptin (TrastuzumAb) (38), Rituxan (RituximAb) (39,40), Campath (AlemtuzumAb) (41), and Mylotarg (GemtuzumAb) (42).

Unlike other EGFR targeting compounds, such as mAbs C225 (43,44) and ABX-EGF (45), or small TKI, such as Iressa (46) and OSI 774 (47), h-R3 did not provoke acneiform rash or folliculitis. The antibody did not cause liver toxicity either, which was expected considering the high EGFR expression in the hepatocytes. Similar results were obtained with the parental, murine mAb, in several patients, in spite of the high cumulative dose used (23,24).

Differences in toxicity are still unclear, but could be associated with the pharmacodynamic and pharmacokinetics properties of the referred compounds. For any drug, effective targeting relies on appropriate pharmacokinetics, ideally showing maximum uptake and retention in tumor and rapid clearance from normal tissue (48). This seemed to be the case of h-R3, where the percentage of ID/g of tissue was significantly higher in malignant lesions than in normal organs, which also showed faster

clearance according to the serial whole-body images. Similar data for other anti-EGFR drugs are not available in the literature, and, in our view, such comparison is warranted. We cannot preclude that the different safety profile could also be explained at cellular or molecular level.

Biodistribution showed the main binding sites of the h-R3, the blood activity profile, and the mAb elimination routes. h-R3 accumulation was seen in liver, heart, kidneys, urinary bladder, spleen, and large intestine. The biodistribution profile agreed with previous reports of our group for the murine antibody (49). Similarities in biodistribution confirmed that after the humanization process, h-R3 maintained the original *in vivo* recognition pattern of normal organs and tissues. The high liver uptake was related with the high EGFR expression in hepatocytes, while the accumulation of the humanized mAb in heart and spleen could be considered as the activity of the vascular compartment. Immune complex formation between the antibody and shed EGFR could also explain the specific accumulation in the spleen. Blood pool activity appeared considerably reduced in the late images. The activity found in kidneys, urinary bladder, and colon illustrated the main excretion routes of the antibody and its metabolites.

Despite the fact that planar or single photon emission computed tomography images were not acquired, positive tumor uptake was observed in five patients (six lesions). The protocol used during the scintigraphic acquisitions was appropriated for biodistribution assessments, but not for lesion imaging. Therefore, the defined matrix format and the scan times provided scintigraphic studies with low statistical counts. As a consequence, low contrast images with minimal usefulness for diagnosis purposes were collected. In addition, since  $^{99m}\text{Tc}$  has a short half-life ( $t_{1/2}$  6.02 hours), the latest images were acquired 24 hours after mAb administration, before optimal tumor/nontumor ratios were achieved, taking into consideration that some tumors have a slow antibody uptake index. Positive tumor visualization was achieved at three of the dosage levels (50, 200, and 400 mg); while at the second lowest dose, tumors were not identified. Malignant lesions in this particular treatment cohort corresponded to two breast carcinomas and a stomach adenocarcinoma, and, therefore, tumor imaging could have been interfered by positive uptake in the vicinity by the liver and the blood pool. Other factors like EGFR expression at the primary tumor as well as the tumor vascularity may also influence mAb uptake.

The use of ior *egf/r3*, the original murine mAb, for radioimmunodetection had already proved to be successful, with 84% of sensitivity for *in vivo* detection of ep-

ithelial tumors from all localizations (25). A diagnostic clinical trial to evaluate the sensitivity, specificity as well as predictive values of h-R3 is ongoing.

$^{99m}\text{Tc}$  was not appropriate for the pharmacokinetics study, because its physical half-life did not match with the antibody clearance. Consequently, an ELISA was developed to quantify h-R3 in serum. However, pharmacokinetics should be considered as preliminary in view of the small number of patients per group. The parameters determined using bi-compartmental analysis suggested a nonlinear behavior of h-R3. The AUC and elimination half-lives increased linearly with dose, while increasing concentrations of the antibody lead to a decrease in plasma clearance between the doses 50 and 200 mg. The peak serum concentrations of h-R3 after infusion were also dose-dependent and its elimination half-life (62.91 to 304.51 hours) was significantly higher than that obtained with the murine mAb (27.3 to 65.89 hours). Similar elimination half-lives had been reported for other chimeric or humanized anti-EGFR antibodies (50,51).

Clearance in cancer patients could be modified by several factors including soluble antigen in circulation. For instance, phase I studies revealed that an increased clearance of Herceptin, was associated with high levels of shed antigen. In our small sample, EGFR shedding did not correlate with h-R3 clearance.

Increased serum ECD levels have been reported in patients with cancers known to overexpress Her 1 or Her 2 (52–54). In our set, soluble EGFR was very high in three patients bearing ductal infiltrating breast carcinomas, while according to the literature, EGFR is only overexpressed in 25–30% of breast carcinomas using immunohistochemistry or Fluorescence in Situ Hybridization (FISH) (55,56). Previously, no significant association had been found between the serum EGFR level and TNM stage, tumor burden or the differentiation degree. Moreover, in some studies, no differences in this oncoprotein serum levels, had been observed in patients with immunohistochemically overexpressing and nonoverexpressing tumors (52–54). The origin and biologic role of soluble EGFR remains to be determined.

The lack of anti-idiotypic response emphasize the relatively nonimmunogenicity of the humanized mAb, although it is necessary to confirm this finding in a larger series of patients treated with repeated doses of h-R3.

In conclusion, h-R3 is a new, promising anti-EGFR antibody. Major advantages of the antibody rely on its reduced toxicity and immunogenicity and on its prolonged half-life. It can be used as a single agent or in combination with radiation or chemotherapy. As radio or chemotherapy may increase EGFR-mediated signal

transduction or expression by tumor cells, the combination seems to be the ideal scenario for the antibody. Completion of the phase II trial using repeated mAb doses in conjunction with radiotherapy is underway to define the response rate in advanced head and neck cancer patients. Further work is in progress to optimize the effects of h-R3 in other tumor localizations.

## REFERENCES

- Brabender J, Danenberg KD, Metzger R, et al. Epidermal growth factor receptor and HER2-neu mRNA expression in non-small cell lung cancer is correlated with survival. *Clin Cancer Res.* 2001;7:1850–1855.
- Nicholson RI, Gee JM, Harper ME. EGFR and cancer prognosis. *Eur J Cancer.* 2001;37(Suppl 4):9–15.
- Liebermann TA, Razon N, Bartal AD, et al. Expression of epidermal growth factor receptors in human brain tumors. *Cancer Res.* 1984;4:753–760.
- Feldkamp MM, Lau N, Guha A. Signal transduction pathways and their relevance in human astrocytomas. *Cancer Immunol Immunother.* 1997;44:157–164.
- Kearsley JH, Leonard JH, Walsh MD, et al. A comparison of epidermal growth factor receptor (EGFR) and c-erbB-2 oncogene expression in head and neck squamous cell carcinomas. *Pathology.* 1991;23:189–194.
- Rikimaru K, Tadokoro K, Yamamoto T, et al. Gene amplification and overexpression of epidermal growth factor receptor in squamous cell carcinoma of the head and neck. *Head Neck.* 1992;14:8–13.
- Alper O, Bergmann-Leitner ES, Bennett TA, et al. Epidermal growth factor receptor signaling and the invasive phenotype of ovarian carcinoma cells. *J Natl Cancer Ins.* 2001;93:1375–1384.
- Bianco C, Bianco R, Tortora G, et al. Antitumor activity of combined treatment of human cancer cells with ionizing radiation and anti-epidermal growth factor receptor monoclonal antibody C225 plus type I protein kinase A antisense oligonucleotide. *Clin Cancer Res.* 2000;6:4343–4350.
- Ngan HY, Cheung AN, Liu SS, et al. Abnormal expression of epidermal growth factor receptor and c-erbB2 in squamous cell carcinoma of the cervix: correlation with human papillomavirus and prognosis. *Tumor Biol.* 2001;22:176–183.
- Chow NH, Chan SH, Tzai TS, et al. Expression profiles of ErbB family receptors and prognosis in primary transitional cell carcinoma of the urinary bladder. *Clin Cancer Res.* 2001;7:1957–1962.
- Inada S, Koto T, Futami K, et al. Evaluation of malignancy and the prognosis of esophageal cancer based on an immunohistochemical study (p53, E-cadherin, epidermal growth factor receptor). *Surg Today.* 1999;29:493–503.
- Wang LS, Chow KC, Chi KH. Prognosis of esophageal squamous cell carcinoma: analysis of clinicopathologic and biologic factors. *Am J Gastroenterol.* 1999;94:1933–1940.
- Giordano A, Rustum YM, Wenner CE. Cell cycle: molecular targets for diagnosis and therapy: tumor suppressor genes and cell cycle progression in cancer. *J Cell Biochem.* 1998;70:1–7.
- Damstrup L, Rude Voldborg B, Spang-Thomsen M, et al. In vitro invasion of small-cell lung cancer cell lines correlates with expression of epidermal growth factor receptor. *Br J Cancer.* 1998;78:631–640.
- Petit AM, Rak J, Hung MC, et al. Neutralizing antibodies against epidermal growth factor and ErbB-2/neu receptor tyrosine kinases downregulate vascular endothelial growth factor production by tumor cells in vitro and in vivo: angiogenic implications for signal transduction therapy of solid tumors. *Am J Pathol.* 1997;151:1523–1530.
- Kerbel RS, Vitoria-Petit A, Okada F, et al. Establishing a link between oncogenes and tumor angiogenesis. *Mol Med.* 1998;4:286–295.
- Gibson S, Tu S, Oyer R, et al. Epidermal growth factor protects epithelial cells against Fas-induced apoptosis. Requirement for Akt activation. *J Biol Chem.* 1999;274:17612–17618.
- Mendelsohn J, Baselga J. The EGF receptor family as targets for cancer therapy. *Oncogene.* 2000;19:6550–6565.
- Kim ES, Khuri FR, Herbst RS. Epidermal growth factor receptor biology (IMC-C225). *Curr Opin Oncol.* 2001;13:506–513.
- Ciardiello F, Tortora G. A novel approach in the treatment of cancer: targeting the epidermal growth factor receptor. *Clin Cancer Res.* 2001;7:2958–70.
- Fernández A, Pérez R, Macías A, et al. Generation and characterization of anti-EGFR antibodies. *Interferon y Biotecnología.* 1989;6:289–298.
- Fernández A, Spitzer E, Pérez R, et al. A new monoclonal antibody for detection of the EGF-R in Western Blot and paraffin embedded tissue sections. *J Cell Biochem.* 1992;49:157–165.
- Crombet T, Torres O, Neninger E, et al. Phase I clinical evaluation of a neutralizing monoclonal antibody against epidermal growth factor receptor. *Cancer Biother Radiopharm.* 2001;16:93–102.
- Crombet T, Torres O, Rodriguez V, et al. Phase I clinical evaluation of a neutralizing monoclonal antibody against epidermal growth factor receptor in advanced brain tumor patients: preliminary study. *Hybridoma.* 2001;20:131–136.
- Ramos-Suzarte M, Rodriguez N, Oliva JP, et al. 99mTc-labeled antihuman epidermal growth factor receptor antibody in patients with tumors of epithelial origin: Part III. Clinical trials safety and diagnostic efficacy. *J Nucl Med.* 1999;40:768–775.
- Mateo C, Moreno E, Amour K, et al. Humanization of a mouse monoclonal antibody that blocks the epidermal growth factor receptor: recovery of antagonistic activity. *Immunotechnology.* 1997;3:71–81.
- Vitoria-Petit A, Crombet T, Jothy S, et al. Acquired resistance to the antitumor effect of epidermal growth factor receptor-blocking antibodies in vivo: a role for altered tumor angiogenesis. *Cancer Res.* 2001;61:5090–5101.
- Crombet-Ramos T, Rak J, Perez R, et al. Antiproliferative, anti-angiogenic and proapoptotic activity of h-R3: A humanized anti-EGFR antibody. *Int J Cancer.* 2002;101:567–575.
- Stragliotto G, Vega F, Stasiecki P et al. Multiple infusions of anti-epidermal growth factor receptor (EGFR) monoclonal antibody (EMD 55,900) in patients with recurrent malignant gliomas. *Eur J Cancer.* 1996;32A:636–640.
- Edwards IR. Harmonisation in pharmacovigilance. *Drug Saf.* 1994;10:93.
- Schwarz A, Steinstraber A. A novel approach to Tc-99m-labeled monoclonal antibodies. *J Nucl Med.* 1987;28:721–727.
- Iznaga Escobar N, Morales AM, Duconge J, et al. Pharmacokinetics, biodistribution and dosimetry of 99mTc-labeled anti-human epidermal growth factor receptor humanized monoclonal antibody R3 in rats. *Nucl Med Biol.* 1998;25:17–23.
- Morales AA, Duconge J, Alvarez-Ruiz D, et al. Humanized versus murine anti-human epidermal growth factor receptor monoclonal antibodies for immunoscintigraphic studies. *Nucl Med Biol.* 2000;27:199–206.
- Macías A, Pérez R, Lage A. Estudios sobre el factor de crecimiento epidérmico (EGF) II: Desarrollo de un radioreceptor analisis para la determinación de cantidades picomolares. *Interferon y Biotecnología.* 1985;2:115–127.
- Akaike A. Posterior probabilities for choosing regression models. *Ann Inst Math Stat.* 1978;30:A9.
- Rosenberg S. Principles of Cancer Management: Biologic Therapy. In: De Vita V, Hellman S, Rosenberg S, eds. *Cancer: Principles and Practice of Oncology 2001.* 6th ed. Philadelphia, PA: Lippincott Williams & Wilkins; 2001:307–334.
- Ciardiello F. Epidermal growth factor receptor tyrosine kinase inhibitors as anticancer agents. *Drugs.* 2000;60(suppl 1):25:41–42.
- Slamon D, Leyland B, Shak S, et al. Use of chemotherapy plus a

- monoclonal antibody against Her 2 for metastatic breast cancer that overexpresses Her 2. *N Engl J Med.* 2000;344:783–792.
39. Davis TA, Grillo-López AJ, White CA, et al. RituximAb anti-CD20 monoclonal antibody therapy in non-Hodgkin's lymphoma: safety and efficacy of re-treatment. *J Clin Oncol.* 2000;18:3135–3143.
  40. Piro LD, White CA, Grillo-Lopez AJ, et al. Extended RituximAb (anti-CD20 monoclonal antibody) therapy for relapsed or refractory low-grade or follicular non-Hodgkin's lymphoma. *Ann Oncol.* 2000;10:655–661.
  41. Dearden CE, Matutes E, Cazin B, et al. High remission rate in T-cell prolymphocytic leukemia with CAMPATH-1H. *Blood.* 2001;98:1721–1726.
  42. Bross PF, Beitz J, Chen G, et al. Approval summary: gemtuzumAb ozogamicin in relapsed acute myeloid leukemia. *Clin Cancer Res.* 2001;7:1490–1496.
  43. Busam KJ, Capodiecchi P, Motzer R, et al. Cutaneous side-effects in cancer patients treated with the anti-epidermal growth factor receptor antibody C225. *Br J Dermatol.* 2001;144:1169–1176.
  44. Shin DM, Donato NJ, Perez-Soler R, et al. Epidermal growth factor receptor-targeted therapy with C225 and cisplatin in patients with head and neck cancer. *Clin Cancer Res.* 2001;7:1204–1212.
  45. Figlin R, Belldgrun A, Lohner M, et al. ABX-EGF: a fully human anti-EGF receptor antibody in patients with advanced cancer [abstract]. *Proc Am Soc Clin Oncol.* 2001;20:276a.
  46. Meric JB, Faivre S, Monnerat C, et al. Zd 1839 “Iressa” *Bull Cancer.* 2000;87:873–876.
  47. Hidalgo M, Siu LL, Nemunaitis J, et al. Phase I and pharmacologic study of OSI-774, an epidermal growth factor receptor tyrosine kinase inhibitor, in patients with advanced solid malignancies. *J Clin Oncol.* 2001;19:3267–3279.
  48. Stroomer JW, Roos JC, Sproll M, et al. Safety and biodistribution of 99mTechnetium-labeled anti-CD44v6 monoclonal antibody BIWA 1 in head and neck cancer patients. *Clin Cancer Res.* 2000; 6:3046–3055.
  49. Iznaga-Escobar N, Torres LA, Morales A, et al. Tm-99m-labeled anti-EGF-receptor antibody in patients with tumor of epithelial origin: I. Biodistribution and dosimetry for radioimmunotherapy. *J Nucl Med.* 1998;15:18–27.
  50. Baselga J, Pfister D, Cooper MR, et al. Phase I studies of anti-epidermal growth factor receptor chimeric antibody C225 alone and in combination with cisplatin. *J Clin Oncol.* 2000;18:904–914.
  51. Bier H, Hoffmann T, Hauser U, et al. Clinical trial with escalating doses of the anti-epidermal growth factor receptor humanized monoclonal antibody EMD 72 000 in patients with advanced squamous cell carcinoma of the larynx and hypopharynx. *Cancer Chemother Pharmacol.* 2001;47:519–524.
  52. Partanen R, Hemminki K, Koskinen H, et al. The detection of increased amounts of the extracellular domain of the epidermal growth factor receptor in serum during carcinogenesis in asbestosis patients. *J Occup Med.* 1994;36:1324–1328.
  53. Choi JH, Oh JY, Ryu SK, et al. Detection of epidermal growth factor receptor in the serum of gastric carcinoma patients. *Cancer.* 1997;79:1879–1883.
  54. Oh MJ, Choi JH, Kim IH, et al. Detection of epidermal growth factor receptor in the serum of patients with cervical carcinoma. *Clin Cancer Res.* 2000;6:4760–4763.
  55. Sharma BK, Ray A, Kaur S, et al. Immunohistochemical co-expression of c-erbB-2/Neu oncoprotein, altered tumor suppressor (p53) protein, EGF-R and EMA in histologic subtypes of infiltrating duct carcinoma of the breast. *Indian J Exp Biol.* 1999;37: 223–227.
  56. Umekita Y, Ohi Y, Sagara Y, et al. Co-expression of epidermal growth factor receptor and transforming growth factor-alpha predicts worse prognosis in breast-cancer patients. *Int J Cancer.* 2000; 89:484–487.